



# Diphenyloctyl phosphate as a solid electrolyte interphase forming additive for Li-ion batteries



In-Jun Park, Tae-Heum Nam, Jung-Gu Kim\*

School of Advanced Materials Science and Engineering, Sungkyunkwan University, 300 Chunchun-Dong, Jangan-Gu, Suwon 440-746, Republic of Korea

## HIGHLIGHTS

- Addition of DPOF in electrolyte improves the rate performance of the lithium ion battery.
- The cell impedance with DPOF is lower than that without DPOF.
- DPOF forms the SEI film composed of  $\text{Li}_3\text{PO}_4$  on the anode electrode.
- $\text{Li}_3\text{PO}_4$  increases the mobility of lithium ion at the interface between anode electrode and electrolyte.

## ARTICLE INFO

### Article history:

Received 12 November 2012

Received in revised form

24 January 2013

Accepted 7 March 2013

Available online 16 March 2013

### Keywords:

Lithium ion battery

Solid electrolyte interphase

Film-forming additive

Diphenyloctyl phosphate

Three-electrode impedance

High rate performance

## ABSTRACT

The cycleability and rate performance of Li-ion batteries are mainly influenced by the characteristics of the solid electrolyte interphase (SEI) film. The use of diphenyloctyl phosphate (DPOF) was investigated as an SEI-forming additive in electrolyte. Cyclic voltammetry (CV), three-electrode electrochemical impedance spectroscopy (EIS), X-ray photoelectron spectroscopy (XPS) and scanning electron microscopy (SEM) were used for the analyzes. The cell with DPOF had better cell performance than that without DPOF in cycle life tests and rate performance tests. In the three-electrode EIS tests, the impedance of the graphite anode electrode of the cell with DPOF was lower than that of the base electrolyte. In the XPS analysis,  $\text{Li}_3\text{PO}_4$ , which is known as inorganic substance that improves lithium ion conductivity, was formed on the SEI film by reduction of DPOF. From these results, the rate performance of the cell with DPOF was improved by the SEI film composed of  $\text{Li}_3\text{PO}_4$ .

© 2013 Elsevier B.V. All rights reserved.

## 1. Introduction

Lithium ion batteries (LIBs) are being successfully used in portable consumer electronics such as cellular phones and notebooks. Recently, intensive research and development on LIB applications have been headed toward electrical storage systems for electric (EV), hybrid (HEV), and plug-in hybrid vehicles (PHEV). These applications are more demanding on the battery and require enhancement of specifications, particularly, increasing the safety, energy densities, cycleability and high-rate performance. Improvement of the high-rate performance of LIBs is especially important for application as an electric storage device for high-power electric vehicles [1–4].

To enhance the rate performance and cycleability of LIBs, the internal resistance induced by lithium ion (charge) transport at an electrode/electrolyte interface, which controls the charge–discharge reaction of LIBs, should be decreased. The desolvation and diffusion of lithium ions through the solid electrolyte interphase (SEI) film are the rate-determining steps of the interfacial lithium ion transfer in graphite [5,6]. To reduce the resistance of lithium diffusion at the interface between electrode and electrolyte, various methods are being investigated, such as development of large-surface-area electrodes using nanosize active materials [7,8], lowering the resistance of electrolytes [9,10], and surface coating of metallic compounds onto electrodes [11,12]. However, commercialization of these methods for LIBs is limited due to complexity and high expenditure. The introduction of additives to the electrolyte is relatively simple and highly applicable to enhance the cell performance of LIBs. In our previous works, although DPOF was studied as a flame retarding additive, it enhanced the thermal

\* Corresponding author. Tel.: +82 31 290 7360; fax: +82 31 290 7410.  
E-mail address: [kimjg@skku.ac.kr](mailto:kimjg@skku.ac.kr) (J.-G. Kim).

safety, cycleability and rate performance of the battery, which can be attributed to the formation of SEI film on the anode electrode by reduction of DPOF [13,14]. In comparison to the existing SEI-forming additives such as VC [15] and VEC [16], the addition of DPOF enhanced the rate performance.

In the present work, the effect of DPOF as an SEI-forming additive in electrolyte for LIB was investigated regarding the rate performance and cycleability of LIBs. Cyclic voltammetry (CV) was used to evaluate the reduction property of DPOF in electrolyte. The effect of SEI film on the internal resistance of LIBs was investigated using three-electrode electrochemical impedance spectroscopy (EIS). The rate performance may result from the internal resistance of the anode electrode, the cathode electrode, and the electrolyte, individually or interactively. However, it is difficult to analyze the phenomena with a prevailing two-electrode system, which cannot differentiate between the impedance of the anode and cathode sides. By using a three-electrode system, it is possible to analyze the phenomena of the anode and the cathode independently [17–20]. The morphology and chemical composition of SEI film induced by reduction of DPOF was also analyzed using X-ray photoelectron spectroscopy (XPS) and scanning electron microscopy (SEM).

## 2. Experimental

Cell performance and EIS tests were performed using a three-electrode pouch-type cell. In the Li-ion cell, mesocarbon microbeads (MCMB),  $\text{Li}(\text{Ni}_{1/3}\text{Mn}_{1/3}\text{Co}_{1/3})\text{O}_2$ , and Li foils were used as the anode, cathode and reference materials, respectively. The electrolyte consisted of 1.15 M  $\text{LiPF}_6$  dissolved in ethylene carbonate and ethyl–methyl carbonate (EC:EMC 4:6 v/v). 1 wt.% of diphenyloctyl phosphate (DPOF) was used as an SEI-forming additive. The compositions of the two different electrolytes are shown in Table 1. All carbonates and lithium salt were obtained from the SOUL BRAIN Company and used without further purification. DPOF (TOKYO CHEMICAL INDUSTRY) was added directly to the base electrolyte. A porous polypropylene film was used to separate the anode and cathode. All cells were assembled in a dry room.

The electrochemical reduction potential of the DPOF-containing electrolyte was measured by CV. The CV test was performed using a three-electrode pouch-type cell with an MCMB electrode ( $6.25 \text{ cm}^2$ ) as the working electrode, and lithium metal foil electrode as the counter electrode ( $5.5 \text{ cm}^2$ ) and the reference electrode ( $0.2 \text{ cm}^2$ ). The potential was scanned between 0 and 2.0 V versus  $\text{Li}/\text{Li}^+$  at a scan rate of  $1 \text{ mV s}^{-1}$ . The CV tests were performed by means of a VMP2 multi-channel potentiostat.

The SEI formation process of the cells with the two different electrolytes was performed at a rate of 0.1 C. The SEI formation process presently used in the manufacture of lithium-ion batteries includes the SEI growth process and lithium ion intercalation process into graphite anode. The rate performance of the cells was evaluated by a constant current discharge at rates of 0.1 C, 1.0 C, and 2.0 C. In the rate performance tests, the cells were charged to 4.2 V with a constant current and constant voltage (CC/CV) protocol at a rate of 0.1 C and then discharged to 2.75 V at different discharge rates.

In order to evaluate the cycleability and the AC impedance change, the cycle-life test and three-electrode EIS test were

performed using cells with DPOF-free and DPOF-containing electrolytes. To evaluate the validity of three-electrode EIS system on lithium ion battery, the sum of the three-electrode measurement value (cathode vs. reference + anode vs. reference) and two-electrode measurement value (anode vs. cathode) was compared (Fig. 1). Less than 2% difference was found between the sum of the three-electrode measurements and the two-electrode measurement in the real part ( $Z_{\text{real}}$ ) of the spectrum, and less than 5% difference in the imaginary region ( $Z_{\text{image}}$ ). This little difference between spectra of two- and three-electrode EIS tests means the validity of three-electrode EIS test.

The charge and discharge cycle-life test was conducted with a VMP2 system at a rate of 1.0 C in the voltage range of 4.2–2.75 V for 30 cycles. Three-electrode impedance measurements of the cells during cycling were performed with the same equipment. The frequency was varied from 100 kHz to 10 mHz and the amplitude was set at 10 mV. Impedance data were fitted by using ZSimpWin Version 3.00 software. All experiments were conducted at room temperature.

To investigate the morphology and the chemical composition on the anode electrode surface, SEM and XPS analyzes were performed both before and after cycle-life test. The anode electrodes were rinsed with dimethyl carbonate (DMC) solution to remove lithium salts. After rinsing, the electrodes were dried for 1 h in an  $\text{N}_2$  charged glove box, and then analyzed.

## 3. Results and discussion

### 3.1. Cyclic voltammetry test

During the first charge of lithium ion battery, electrolyte is decomposed to organic and inorganic specimens by reduction reaction at the anode electrode. These decomposed specimens absorb on the electrode surface and construct the SEI film [20]. Therefore, the reduction potential of electrolyte plays an indicator role in the start point of SEI film formation. To evaluate the reduction potential of the two electrolytes, CV tests were carried out in the potential range of 2.0 to 0 V vs.  $\text{Li}/\text{Li}^+$ , as shown in Fig. 2. The current value,  $-0.1 \text{ mA cm}^{-2}$ , was used as a reference point to clearly measure the onset potential of the reduction reaction. In the first cycle, the reduction potentials of E1 and E2 were observed at about 0.87 and 1.02 V vs.  $\text{Li}/\text{Li}^+$  at  $-0.1 \text{ mA cm}^{-2}$ . It is shown that the preferential reduction of DPOF appears to favor SEI formation. With

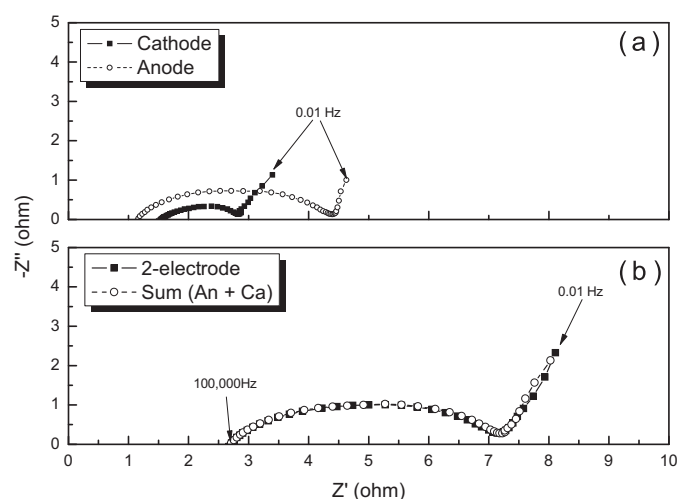


Fig. 1. Impedance spectra at 3.6 V: (a) The anode/cathode electrodes and (b) 2-electrode system/the sum of the two-electrode impedance of E1.

Table 1  
Electrolyte compositions.

Electrolyte	Composition
E1	1.15 M $\text{LiPF}_6$ EC:EMC (4:6, v/v)
E2	1.15 M $\text{LiPF}_6$ EC:EMC (4:6, v/v) + DPOF 1% (w/w)

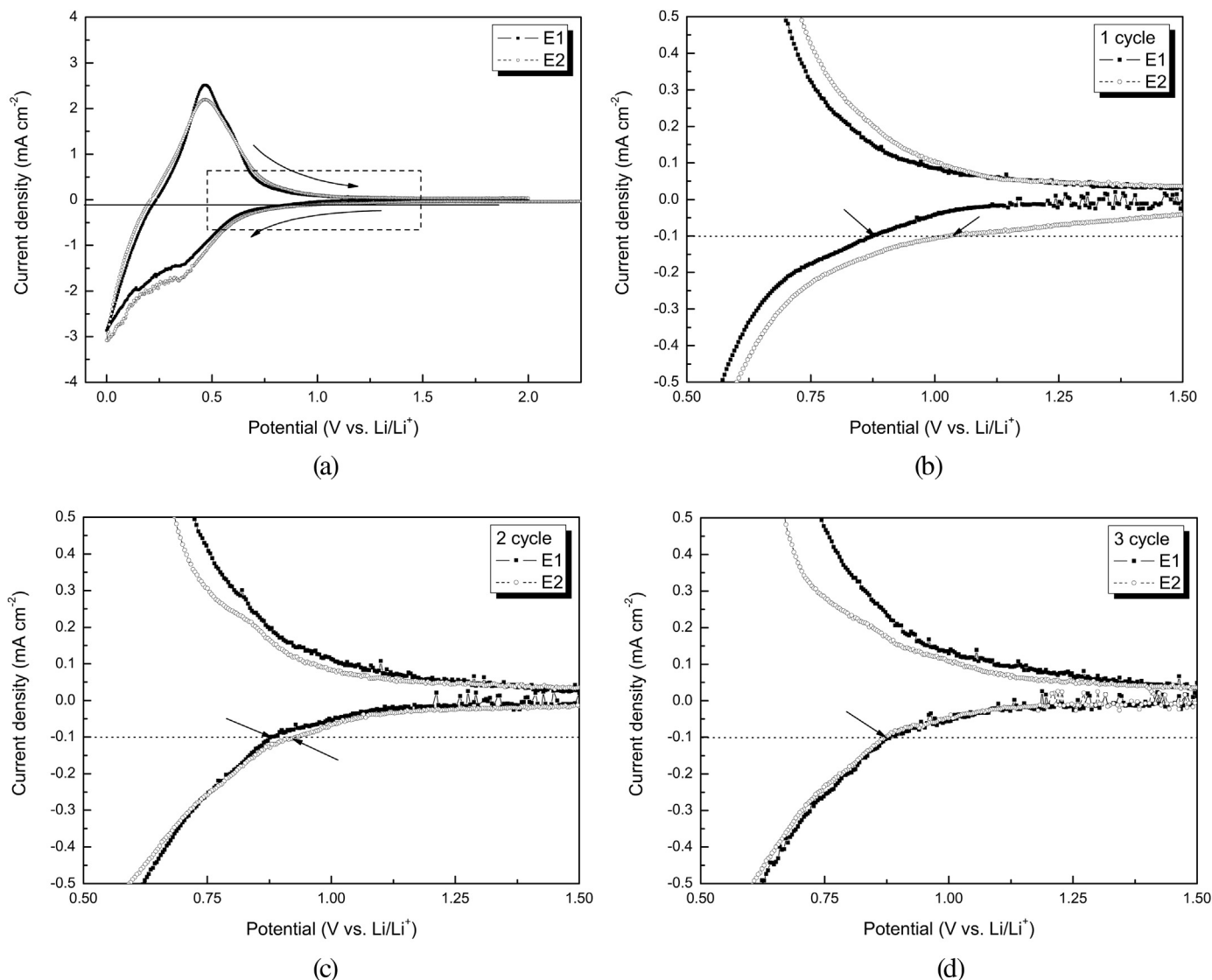


Fig. 2. Cyclic voltammograms of two electrolytes: (a, b) 1st cycle, (c) 2nd cycle, (d) 3rd cycle.

increasing cycle number, the reduction voltage of E2 was shifted to lower value (0.92 V), and was finally overlapped with E1 in the third cycle (0.87 V). These results indicate that DPOF was reduced and consumed during cycle. In short, the effective SEI formation progresses by reduction of DPOF before that of base electrolyte.

### 3.2. Cell performance

In order to satisfy the demands of high-power applications, Li-ion cells must deliver good performance at high current drains. The variation of capacity at high rate can be affected by several processes in the cell, such as the ionic conductivity within the electrode, and the diffusion and migration processes of lithium ions in the SEI layer. From these reaction steps, lithium ion exchange is known as the rate-determining step at the interface between electrode and electrolyte when battery is working [21,22]. Namely, lithium ion exchange rate at the interface affects the rate capability of lithium ion battery. The rate performance of the cells under different discharge rates is given in Fig. 3. Both the capacity and voltage decreased with increasing discharge rate, due to the IR drops at the electrode–electrolyte interface and in the electrolyte [23].

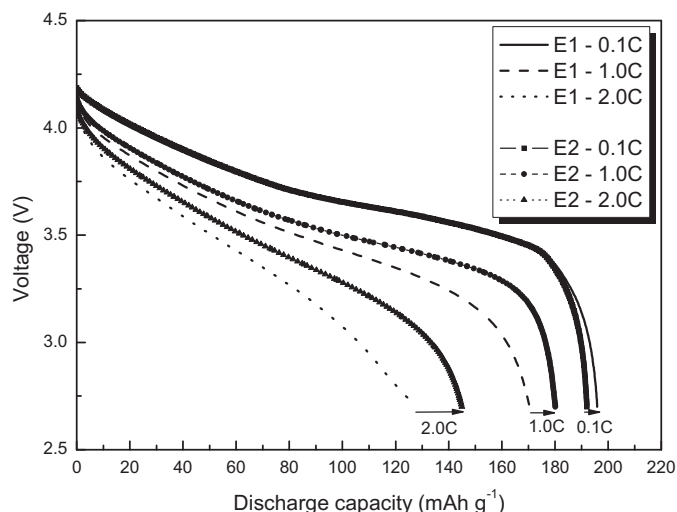
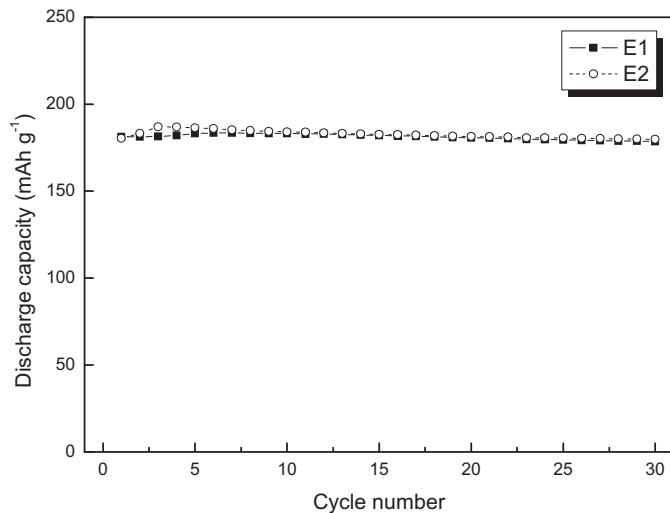


Fig. 3. Discharge curves of cells with two electrolytes at 0.1 C, 1.0 C and 2.0 C.



**Fig. 4.** Specific discharge capacities as a function of cycle number for the cells with two electrolytes at 1.0 C rate.

The E1 cell exhibited rate performance of 64.95% at 2.0 C, and the E2 cell showed better rate performance of 75.55% at a rate of 2.0 C. The cell of E2 with DPOF shows a higher rate capability than E1. From these results, it is thought that DPOF improves the lithium ion exchange rate at the electrode–electrolyte interface by forming an especial SEI film.

Fig. 4 shows the electrochemical cycling performance of the two cells at room temperature. The electrochemical cycle-life test of the cells was carried out at a constant rate of 1.0 C within a voltage

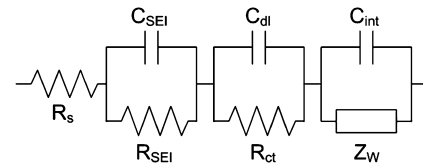


**Fig. 6.** Equivalent circuit used to analyze impedance spectra.

range of 2.75–4.2 V. The cell with the E1 and E2 showed capacity retention of about 98.53% and 99.65% of the initial capacity after 30 cycles, respectively. Although E2 shows about one percent improvement of capacity retention than E1 at 30 cycles, the cell contained DPOF has a better cycleability than the cell which is not contained DPOF with considering our previous results [13,14].

It is reported that VC forms the SEI film on the anode electrode which improves the cycleability of lithium ion battery [15]. However, effect of VC on the rate capability of lithium ion battery was not reported yet. In contrast, addition of DPOF shows the improvement of the cycleability and the rate capability in this study.

### 3.3. Three-electrode EIS measurements

The impedance spectra at 3.6 V of the cell during cycling in the E1 and E2 containing DPOF are shown in Fig. 5. An equivalent circuit used for the EIS analysis is shown in Fig. 6. The EIS of the Li-ion cell is composed of two partially overlapped semicircles and a straight slopping line at the low frequency end [24].  $R_s$  is the electrolyte resistance, while  $R_{SEI}$  and  $C_{SEI}$  are the resistance and capacitance of the SEI film formed on the surface of the electrode, which

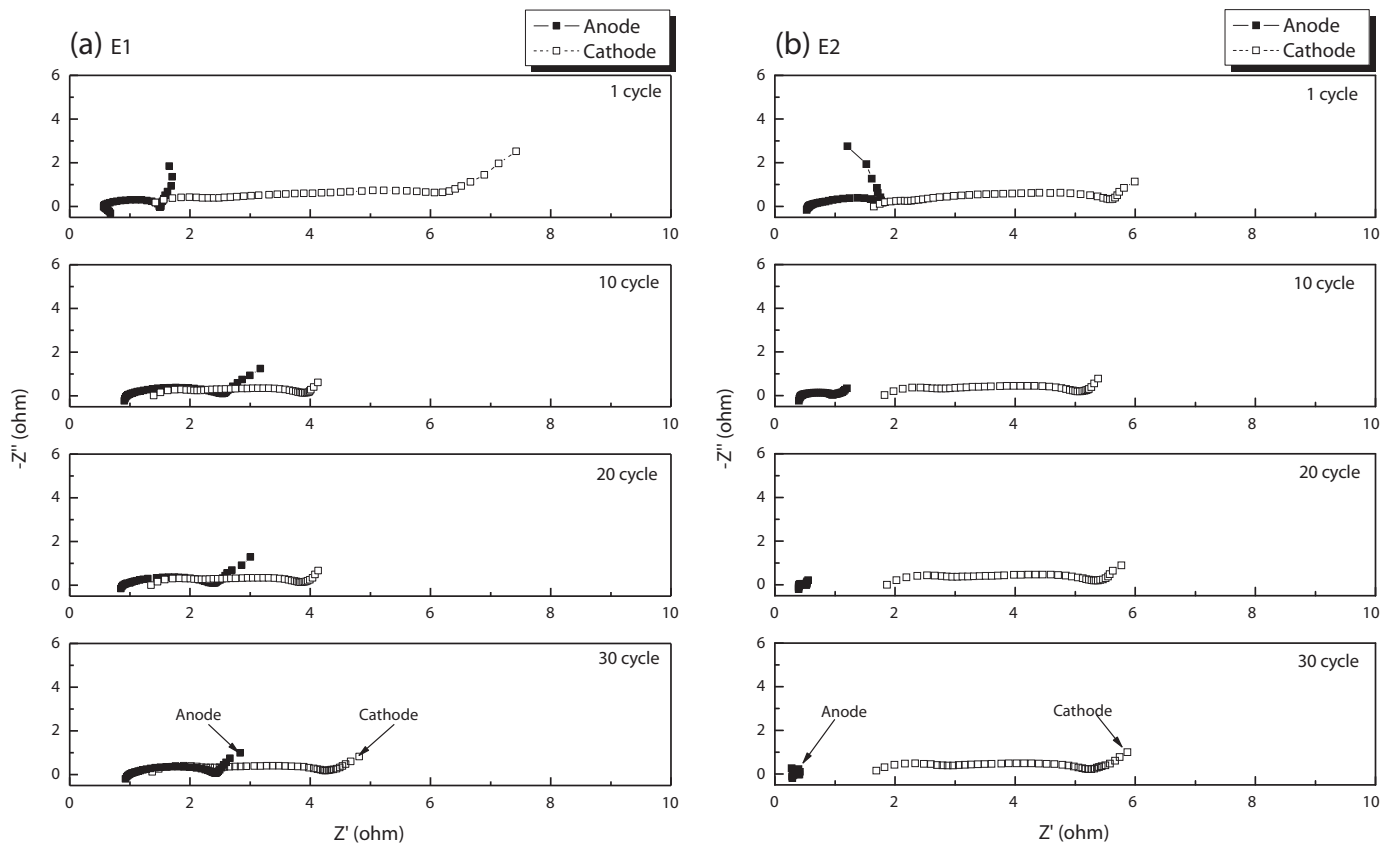
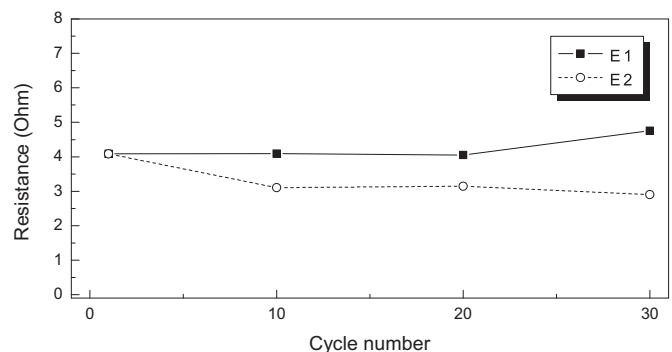


**Fig. 5.** Nyquist plots of (a) E1 and (b) E2 at different cycle numbers.

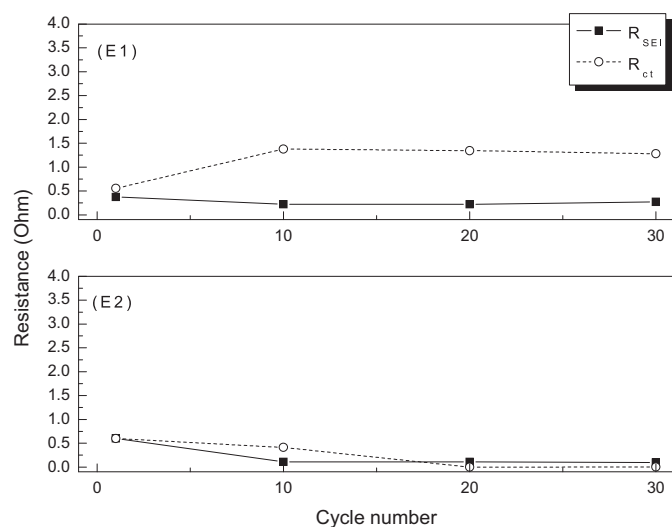
correspond to the semicircle at high frequencies.  $R_{ct}$  and  $C_{dl}$  are the charge-transfer resistance and the double-layer capacitance, respectively, which correspond to the semicircle at medium frequencies.  $W$  and  $C_{int}$  are the Warburg impedance and internal capacitance, respectively, which are related to the combined effect of the diffusion of lithium ions into the active materials of the

electrodes.  $R_{SEI}$  and  $R_{ct}$ , the resistance of the SEI film and charge-transfer, are the most dominant factors of the internal cell resistance [24,25].

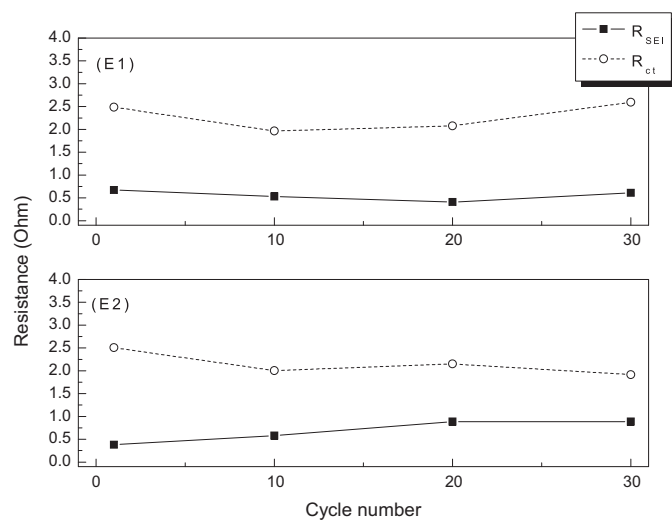
The total resistance,  $R_{SEI}$  and  $R_{ct}$  of the anode and cathode electrode are shown in Fig. 7. The resistance values were directly fitted from the EIS results. As indicated in Fig. 7(a), the total resistance of the E1 cell is increased during the cycleability test, while that of the E2 cell is decreased. Fig. 7(b) shows that  $R_{SEI}$  and  $R_{ct}$  on the anode electrode of the E2 cell are much smaller than those of the E1 cell. On the other hand, there is little difference of the  $R_{SEI}$  and  $R_{ct}$  on the cathode electrodes between the E1 and E2 cells (Fig. 7(c)). Therefore,  $R_{anode}$  ( $R_{SEI} + R_{ct}$  of the anode electrode) is the main reasons for the decrease in total resistance of the E2 cell. The low values of  $R_{anode}$  of the E2 cell confirm that DPOF-containing E2 formed SEI film, which has high lithium ion conductivity on the



(a)



(b)



(c)

Fig. 7. Internal resistance values as a function of the cycle number: (a) Total resistance, (b) Anode electrode and (c) cathode electrode.

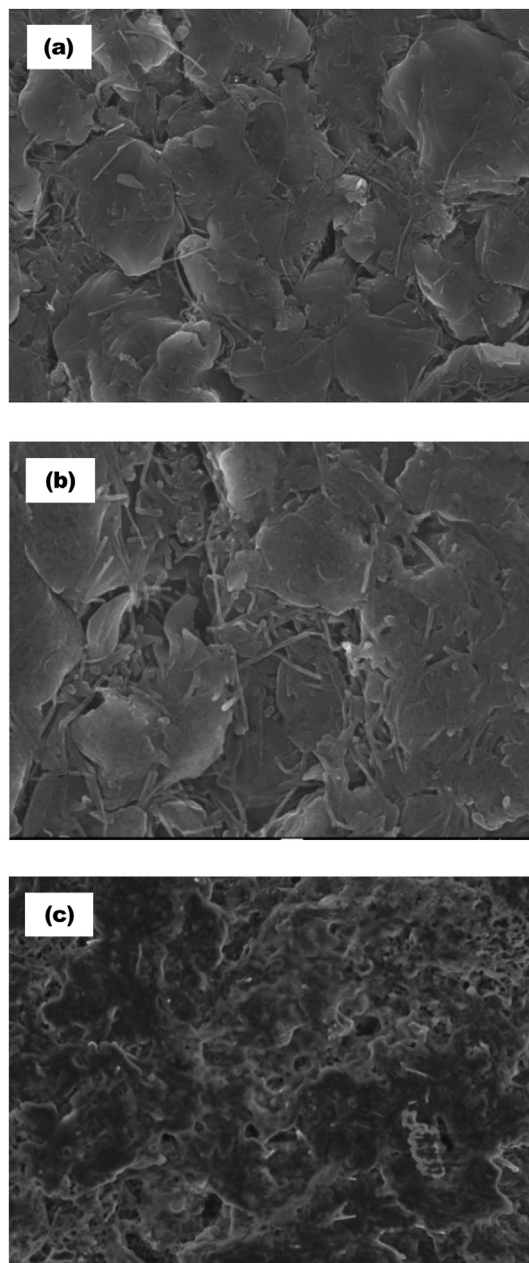
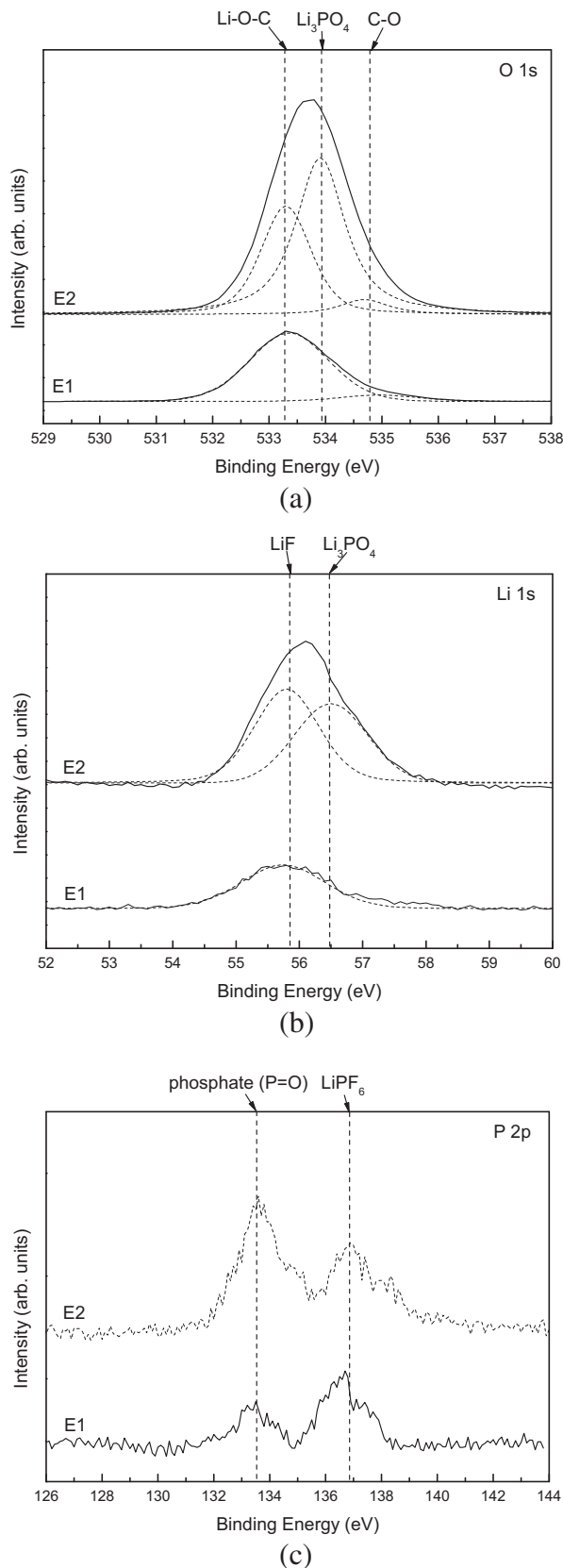


Fig. 8. SEM micrographs of the anode electrodes before and after SEI formation process: (a) Pristine, (b) E1 and (c) E2.





**Fig. 9.** XPS spectra of the anode electrodes after SEI formation process: (a) O 1s, (b) Li 1s and (c) P 2p.

anode electrode. Better rate performance of the E2 cell may come from lower  $R_{\text{anode}}$  of the E2 cell than that of the E1 cell.

### 3.4. SEM analysis

In order to investigate the effect of the DPOF on the electrode morphology before and after the SEI formation cycle, SEM micrographs of the anode electrode were observed and presented in Fig. 8. The micrograph of pristine anode electrode and base electrolyte (E1) electrode are shown in Fig. 8(a) and (b), respectively. It was known that about 5 nm thickness of SEI was formed under similar conditions to the E1 [26], in this study there were but little difference of SEM images between pristine and electrode containing base electrolyte (E1). The micrograph of the E2 electrode (Fig. 8(c)) clearly displays a very different structural shape compared to that of the E1 electrode (Fig. 8(b)). The layer was observed on the electrode containing DPOF (E2), it was known that the film was derived from the diphenyl and phosphate of DPOF [2,13,14]. Therefore, it is assumed that SEI film could be formed on anode electrode due to the reduction reaction of DPOF (Fig. 8(c)).

### 3.5. XPS analysis

XPS analysis was used to evaluate the chemical compositions of SEI film formed on the electrodes after the SEI formation process. Fig. 9 shows O 1s and Li 1s core peaks of the anode electrode after the SEI formation process in two electrolytes. The O 1s spectrum of E1 (Fig. 9(a)) exhibits a main peak of the Li–O–C bond (533.3 eV) and a weak peak of the C–O bond (534.8 eV), indicating lithium alkyl carbonates such as  $\text{ROCO}_2\text{Li}$  and  $\text{R-CH}_2\text{-OCO}_2\text{Li}$  [27,28]. The O 1s spectrum of E2 shows a specific peak of Li–O–P binding energy at 533.9 eV, which could be explained by the presence of  $\text{Li}_3\text{PO}_4$  as a known lithium ion conductive material [29,30]. The Li 1s spectrum of E1 has only one peak at 55.8 eV attributed to LiF, which becomes the main component of the outer part of the SEI (Fig. 9(b)). However, E2 shows the LiF peak and the peak of  $\text{Li}_3\text{PO}_4$  at 56.5 eV. The P 2p spectrum of two samples was shown in Fig. 9(c). The first peak at 137.2 eV is attributed to  $\text{LiPF}_6$  and the second one at 134.3 eV corresponds to the presence of phosphates due to the decomposition of  $\text{LiPF}_6$  and DPOF [31]. The  $\text{LiPF}_6$  peaks (137.2 eV) of E1 and E2 show similar intensity, but the phosphates peak (134.3 eV) intensity of E2 is higher than that of E1. This result indicates DPOF decomposition leads to more phosphates substances on the anode electrode. It is reported that these phosphates can be present in different forms such as  $\text{PO}_4^{3-}$  ions or  $\text{OP(OR)}_3$  where R is an alkyl chain [32]. Although characterization of these phosphates is rather difficult by XPS, the peak of phosphates containing  $\text{PO}_4^{3-}$  can suggest the presence of  $\text{Li}_3\text{PO}_4$ .

$\text{Li}_3\text{PO}_4$  is known as an inorganic substance that improves lithium ion conductivity, and has been studied for application as a solid electrolyte in LIBs [29] and lithium ion sensor membranes [30].  $\text{Li}_3\text{PO}_4$ -contained SEI film was formed by reduction reaction of DPOF, which enhanced the cycleability and rate performance of the cell.

## 4. Conclusions

The effect of DPOF as a functional additive in a liquid electrolyte and usefulness of the three-electrode EIS test have been investigated. The DPOF-containing electrolyte was preferentially reduced rather than the base electrolyte, forming the protective SEI film on the anode electrode. In the cycling tests, a cell with the DPOF-containing electrolyte has better discharge capacity and capacity retention than a cell without DPOF. Through the three-electrode EIS test, it could be verified that the SEI film formed by reduction of DPOF enhanced the migration rate of lithium ions between the

anode electrode and the electrolyte of the cell. In the XPS analysis, the SEI film is composed of DPOF,  $\text{Li}_3\text{PO}_4$  which improves lithium ion conductivity.

### Acknowledgments

This research was supported by the Basic Science Research Program through the National Research Foundation of Korea (NRF), funded by the Ministry of Education, Science and Technology (2010-0022972). Receipt of the electrolyte from SOUL BRAIN Co., Ltd. is gratefully acknowledged.

### References

- [1] D. Aurbach, B. Markovsky, G. Salitra, E. Markevich, Y. Talyossef, M. Koltypin, L. Nazar, B. Ellis, D. Kovacheva, J. Power Sources 165 (2007) 491–499.
- [2] L. Xiao, X. Ai, Y. Cao, H. Yang, Electrochim. Acta 49 (2004) 4189–4196.
- [3] X.L. Yao, S. Xie, C.H. Chen, Q.S. Wang, J.H. Sun, Y.L. Li, S.X. Lu, J. Power Sources 144 (2005) 170–175.
- [4] T.F. Yi, Y. Xie, Q. Wu, H. Liu, L. Jiang, M. Ye, R. Zhu, J. Power Sources 214 (2012) 220–226.
- [5] Y. Yamada, Y. Iriyama, T. Abe, Z. Ogumi, Langmuir 25 (2009) 12766–12770.
- [6] K. Xu, Y. Lam, S.S. Zhang, T.R. Jow, T.B. Curtis, J. Phys. Chem. C 111 (2007) 7411–7421.
- [7] C.H. Lu, T.Y. Wu, H.C. Wu, M.H. Yang, Z.Z. Guo, I. Taniguchi, Mater. Chem. Phys. 112 (2008) 115–119.
- [8] D. Wang, H. Buqa, M. Crouzet, G. Deghenghi, T. Drezen, I. Exnar, N.H. Kwon, J.H. Miners, L. Poletto, M. Grätzel, J. Power Sources 189 (2009) 624–628.
- [9] Y. Abu-Lebdeh, I. Davidson, J. Power Sources 189 (2009) 576–579.
- [10] Z. Chen, W.Q. Lu, J. Liu, K. Amine, Electrochim. Acta 51 (2006) 3322–3326.
- [11] Y. Takahashi, S. Tode, A. Kinoshita, H. Fujimoto, I. Nakane, S. Fujitani, J. Electrochem. Soc. 155 (2008) A537–A541.
- [12] M.R. Yang, W.H. Ke, J. Electrochem. Soc. 155 (2008) A729–A732.
- [13] T.H. Nam, E.G. Shim, J.G. Kim, H.S. Kim, S.I. Moon, J. Power Sources 180 (2008) 561–567.
- [14] E.G. Shim, T.H. Nam, J.G. Kim, H.S. Kim, S.I. Moon, J. Power Sources 175 (2008) 533–539.
- [15] D. Aurbach, K. Gamolsky, B. Markovsky, Y. Gofer, M. Schmidt, U. Heider, Electrochim. Acta 47 (2002) 1423–1439.
- [16] Z. Wang, Y. Hu, L. Chen, J. Power Sources 146 (2005) 51–57.
- [17] J.Y. Song, H.H. Lee, Y.Y. Wang, C.C. Wan, J. Power Sources 111 (2002) 255–267.
- [18] M.S. Wu, P.C. Julia Chiang, Electrochim. Acta 52 (2007) 3719–3725.
- [19] G. Nagasubramanian, J. Power Sources 87 (2000) 226–229.
- [20] E. Peled, J. Electrochem. Soc. 126 (1979) 2047–2051.
- [21] J. Shim, R. Kostecki, T. Richardson, X. song, K.A. Striebel, J. Power Sources 112 (2002) 222–230.
- [22] E. Peled, D. Golodnitsky, G. Ardel, J. Electrochem. Soc. 144 (1997) L208–L210.
- [23] S.S. Zhang, K. Xu, T.R. Jow, J. Power Sources 140 (2005) 361–364.
- [24] S.S. Zhang, K. Xu, T.R. Jow, Electrochim. Acta 49 (2004) 1057–1061.
- [25] S. Yang, H. Song, X. Chen, Electrochem. Commun. 8 (2006) 137–142.
- [26] R. Dedryvère, H. Martinez, S. Leroy, D. Lemordant, F. Bonhomme, P. Biensan, D. Gonbeau, J. Power Sources 174 (2007) 462–468.
- [27] A. Chagnes, B. Carré, P. Willmann, R. Dedryvère, D. Gonbeau, D. Lemordant, J. Electrochem. Soc. 150 (2003) A1255–A1261.
- [28] D. Aurbach, Y. Ein-Eli, B. Markovsky, A. Zaban, S. Luski, Y. Carmeli, H. Yamin, J. Electrochem. Soc. 142 (1995) 2882–2889.
- [29] N.S. Roh, S.D. Lee, H.S. Kwon, Scripta Mater. 42 (2000) 43–49.
- [30] S.Q. Zhang, S. Xie, C.H. Chen, Mater. Sci. Eng. B 121 (2005) 160–165.
- [31] S. Leroy, F. Blanchard, R. Dedryvère, H. Martinez, B. Carré, D. Lemordant, D. Gonbeau, Surf. Interface Anal. 37 (2005) 773–781.
- [32] R. Dedryvère, S. Laruelle, S. Grugeon, L. Gireaud, J.M. Tarascon, D. Gonbeau, J. Electrochem. Soc. 152 (2005) A689–A696.